Article

Activation of C–H / H–H Bonds by Rhodium(II) Porphyrin Bimetalloradicals

Weihong Cui, and Bradford B. Wayland

J. Am. Chem. Soc., **2004**, 126 (26), 8266-8274• DOI: 10.1021/ja049291s • Publication Date (Web): 11 June 2004

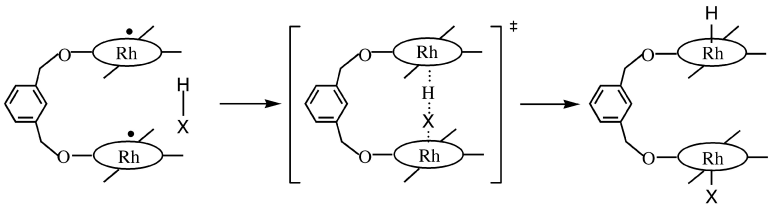

More About This Article

Additional resources and features associated with this article are available within the HTML version:

- Supporting Information
- Links to the 7 articles that cite this article, as of the time of this article download
- Access to high resolution figures
- Links to articles and content related to this article
- Copyright permission to reproduce figures and/or text from this article

View the Full Text HTML

J|A|C|S
ARTICLES
Published on Web 06/11/2004

Activation of C−H / H−H Bonds by Rhodium(II) Porphyrin Bimetalloradicals

Weihong Cui and Bradford B. Wayland*

Contribution from the Department of Chemistry, University of Pennsylvania, Philadelphia, Pennsylvania 19104-6323

Received February 9, 2004; E-mail: wayland@sas.upenn.edu

Abstract: Reactivity, kinetic, and thermodynamic studies are reported for reactions of a rhodium(II) bimetalloradical with H_2, and with the methyl C−H bonds for a series of substrates CH_3R (R = H, CH_3, OH, C_6H_5) using a *m*-xylyl diether tethered diporphyrin ligand. Bimolecular substrate reactions involving the intramolecular use of two metalloradical centers and preorganization of the four-centered transition state (M•···X···Y•···M) result in large rate enhancements as compared to termolecular reactions of monometalloradicals. Activation parameters and deuterium kinetic isotope effects for the substrate reactions are reported. The C−H bond reactions become less thermodynamically favorable as the substrate steric requirements increase, and the activation free energy ($\Delta G^{\ddagger}$) decreases regularly as ΔG° becomes more favorable. An absolute Rh−H bond dissociation enthalpy of 61.1 ± 0.4 kcal mol^{-1} is directly determined, and the derived Rh−CH_2R BDE values increase regularly with the increase in the C−H BDE.

Introduction

Metalloradical reactions of hydrocarbon H−CH_2R bond units with rhodium(II) porphyrins such as (tetramesitylporphyrinato)-rhodium(II) ((TMP)Rh•) result in concerted one-electron oxidative additions of the hydrogen(H•) and organo (•CH_2R) fragments with two metal centers ($2M\bullet + H{-}CH_2R \rightleftharpoons M{-}H + M{-}CH_2R$).[1−6] Rhodium(II) porphyrins are particularly unusual because they react with alkane hydrocarbons and totally exclude aromatic C−H bond activation.[1−6] This selectivity for alkane over aromatic reactivity is kinetic in origin[2] and opposite to other metal systems which typically react with kinetic and thermodynamic preference for aromatic C−H bond reaction.[7−19] Oxidative addition of hydrocarbon C−H units requires an electronically and coordinately unsaturated metal center that usually necessitates generation of the active species by either reductive elimination of a substrate or ligand dissociation.[7−11] The rhodium(II) metalloradical center in rhodium(II) porphyrins functions as a weak Lewis acid and in nondonor media provides an open site for substrate one-electron oxidative addition reactions.[1−6,20] Direct observation of the reactive metal-centered radicals facilitates kinetic studies for the actual substrate bond cleavage event and evaluation of absolute thermodynamic parameters.

Metalloradical reactions of hydrogen[21−23] and hydrocarbons[1−6] occur through a termolecular transition state that contains two metalloradicals and the substrate (M•···H···X···•M; $\text{rate}_f = k[M\bullet]^2[S]$). A near linear four-centered transition state for oxidative addition of H−X with two separate metalloradicals is complementary to the three- and four-centered cyclic transition states implicated in oxidative addition to single metal centers

(1) Sherry, A. E.; Wayland, B. B. *J. Am. Chem. Soc.* **1990**, *112*, 2, 1259.
(2) Wayland, B. B.; Ba, S.; Sherry, A. E. *J. Am. Chem. Soc.* **1991**, *113*, 3, 5305.
(3) Zhang, X.-X.; Wayland, B. B. *J. Am. Chem. Soc.* **1994**, *116*, 7897.
(4) Cui, W.; Zhang, X. P.; Wayland, B. B. *J. Am. Chem. Soc.* **2003**, *125*, 4994.
(5) Nelson, A. P.; DiMagno, S. G. *J. Am. Chem. Soc.* **2000**, *122*, 8569.
(6) (a) Wayland, B. B.; Del Rossi, K. J. *J. Organomet. Chem.* **1984**, *276*, C27. (b) Del Rossi, K. J.; Wayland, B. B. *J. Am. Chem. Soc.* **1985**, *107*, 7, 7941.
(7) Jones, W. D. *Top. Organomet. Chem.* **1999**, *3*, 9.
(8) (a) Jones, W. D.; Feher, F. J. *Acc. Chem. Res.* **1989**, *22*, 2, 91. (b) Jones, W. D.; Feher, F. J. *J. Am. Chem. Soc.* **1984**, *106*, 6, 1650. (c) Jones, W. D.; Feher, F. J. *J. Am. Chem. Soc.* **1986**, *108*, 16, 4814.
(9) (a) Jones, W. D.; Hessell, E. T. *J. Am. Chem. Soc.* **1992**, *114*, 15, 6087. (b) Hessell, E. T.; Jones, W. D. *Organometallics* **1992**, *11*, 1496. (c) Jones, W. D.; Hessell, E. T. *J. Am. Chem. Soc.* **1993**, *115*, 2, 554.
(10) (a) Janowicz, A. H.; Bergman, R. G. *J. Am. Chem. Soc.* **1982**, *104*, 352. (b) Janowicz, A. H.; Bergman, R. G. *J. Am. Chem. Soc.* **1983**, *105*, 12, 3929.
(11) (a) Bergman, R. G. *Adv. Chem. Ser.* **1992**, *230*, 211. (b) Bergman, R. G. *Science* **1984**, *223*, 902.
(12) (a) Hoyano, J. K.; Graham, W. A. G. *J. Am. Chem. Soc.* **1982**, *104*, 3723. (b) Ghosh, C. K.; Graham, W. A. G. *J. Am. Chem. Soc.* **1987**, *109*, 4726.
(13) (a) Labinger, J. A.; Bercaw, J. E. *Nature* **2002**, *417*, 507. (b) Fekl, U.; Goldberg, K. I. *Adv. Inorg. Chem.* **2003**, *54*, 259. (c) Jensen, M. P.; Wick, D. D.; Reinartz, S.; White, P. S.; Templeton, J. L.; Goldberg, K. I. *J. Am. Chem. Soc.* **2003**, *125*, 8614. (d) Norris, C. M.; Reinartz, S.; White, P. S.; Templeton, J. L. *Organometallics* **2002**, *21*, 5649. (e) Reinartz, S.; White, P. S.; Brookhart, M.; Templeton, J. L. *J. Am. Chem. Soc.* **2001**, *123*, 12724.
(14) (a) Thompson, M. E.; Bercaw, J. E. *Pure Appl. Chem.* **1984**, *56*, 1. (b) Thompson, M. E.; Baxter, S. M.; Bulls, A. R.; Burger, B. J.; Nolan, M. C.; Santarsiero, B. D.; Schaefer, W. P.; Bercaw, J. E. *J. Am. Chem. Soc.* **1987**, *109*, 203.
(15) Johansson, L.; Tilset, M.; Labinger, J. A.; Bercaw, J. E. *J. Am. Chem. Soc.* **2000**, *122*, 10846.
(16) (a) Schaller, C. P.; Cummins, C. C.; Wolczanski, P. T. *J. Am. Chem. Soc.* **1996**, *118*, 591. (b) Schaller, C. P.; Wolczanski, P. T. *Inorg. Chem.* **1993**, *32*, 131.
(17) (a) Bennett, J. L.; Wolczanski, P. T. *J. Am. Chem. Soc.* **1994**, *116*, 2179. (b) Bennett, J. L.; Wolczanski, P. T. *J. Am. Chem. Soc.* **1997**, *119*, 10696.
(18) Shilov, A. E.; Shul'pin, G. B. *Chem. Rev.* **1997**, *97*, 2879.
(19) (a) Aoyama, Y.; Yoshida, T.; Sakurai, K.; Ogoshi, H. *J. Chem. Soc., Chem. Commun.* **1983**, 478. (b) Aoyama, Y.; Yoshida, T.; Sakurai, K.; Ogoshi, H. *Organometallics* **1986**, *5*, 168.
(20) Wayland, B. B.; Sherry, A. E.; Bunn, A. G. *J. Am. Chem. Soc.* **1993**, *115*, 7675.
(21) Wayland, B. B.; Ba, S.; Sherry, A. E. *Inorg. Chem.* **1992**, *31*, 148.
(22) (a) Halpern, J.; Pribanic, M. *Inorg. Chem.* **1970**, *9*, 2616. (b) Halpern, J. *Inorg. Chim. Acta* **1982**, *62*, 31. (c) Halpern, J. *Inorg. Chim. Acta* **1983**, *77*, L105.
(23) (a) Capps, K. B.; Bauer, A.; Kiss, G.; Hoff, C. D. *J. Organomet. Chem.* **1999**, *586*, 23. (b) Hoff, C. D. *Coord. Chem. Rev.* **2000**, *206−207*, 451.

10.1021/ja049291s CCC: $27.50

Table 1. Characteristic ^{1}H NMR Shifts (ppm) of the *m*-Xylyl Tethered Dirhodium Diporphyrin Derivatives Useful in the Identification of Species in Solution[a]

complex	tether $-CH_2-$	Rh–X
·Rh(*m*-xylyl)Rh· (**1**)	6.21	
H−Rh(*m*-xylyl)Rh−H (**2**)	4.99	−40.06 (Rh−*H*)
·Rh(*m*-xylyl)Rh−H (**3**)	5.90, 5.31	−40.03 (Rh−*H*)
H_3C−Rh(*m*-xylyl)Rh−CH_3 (**4**)	5.00	−5.29 (Rh−*CH_3*)
·Rh(*m*-xylyl)Rh−CH_3 (**5**)	5.90, 5.31	−5.27 (Rh−*CH_3*)
H−Rh(*m*-xylyl)Rh−CH_3 (**6**)	5.00	−40.06 (Rh−*H*), −5.29 (Rh−*CH_3*)
H−Rh(*m*-xylyl)Rh−CH_2CH_3 (**7**)	5.00	−40.06 (Rh−*H*), −3.89 (Rh−CH_2*CH_3*), −4.33 (Rh−*CH_2*CH_3)
·Rh(*m*-xylyl)Rh−CH_2CH_3 (**8**)	5.90, 5.31	−3.87 (Rh−CH_2*CH_3*), −4.32 (Rh−*CH_2*CH_3)
CH_3CH_2−Rh(*m*-xylyl)Rh−CH_2CH_3 (**9**)	5.00	−3.89 (Rh−CH_2*CH_3*), −4.33 (Rh−*CH_2*CH_3)
H−Rh(*m*-xylyl)Rh−CH_2OH (**10**)	5.00, 5.01	−40.06 (Rh−*H*), −1.61 (Rh−*CH_2*OH), −4.16 (Rh−CH_2*OH*)
·Rh(*m*-xylyl)Rh−CH_2OH (**11**)	5.90, 5.31	−1.60 (Rh−*CH_2*OH), −4.15 (Rh−CH_2*OH*)
$HOCH_2$−Rh(*m*-xylyl)Rh−CH_2OH (**12**)	5.01	−1.60 (Rh−*CH_2*OH), −4.13 (Rh−CH_2*OH*)
$PhCH_2$−Rh(*m*-xylyl)Rh−CH_2Ph (**13**)	5.04	−3.21 (Rh−*CH_2*Ph)
·Rh(*m*-xylyl)Rh−CH_2Ph (**14**)	5.90, 5.36	−3.17 (Rh−*CH_2*Ph)
H−Rh(*m*-xylyl)Rh−CH_2Ph (**15**)	4.99, 5.04	−40.06 (Rh−*H*), −3.20 (Rh−*CH_2*Ph)

[a] C_6D_6 solvent (T = 296 K); complete ^{1}H NMR data are reported in the Supporting Information.

(M),[7−11] and addition to M−X[14,24] and M═X bonds.[16,17,25] These types of transition states synchronize the H−X bond breaking with the formation of two bonds, which is necessary to have low energy pathways for processes where the bond that is being broken is substantially stronger than either of the bonds being formed. Elegant mechanistic studies for two-electron oxidative addition of hydrocarbon C−H bonds to a metal center through the intermediacy of hydrocarbon σ complexes have revealed a labyrinth of reaction pathways with subtle variations.[26,27] In comparison, there is no evidence at present for complexities of these types in the rhodium(II) porphyrin metalloradical reactions with hydrocarbons. The electronic structure for rhodium(II) in the strong square-planar ligand field imposed by the porphyrin is not conducive to hydrocarbon complex formation, and the steric requirements of the porphyrin also restrict the range of the transition state structures.

Termolecular reactions are inherently slow, and one strategy to obtain rate enhancements is to tether two metalloradical sites into a molecular unit where the metalloradicals can reach the transition state for substrate C−H bond reactions.[3,4,29,30] This Article reports on reactivity, kinetic, and thermodynamic studies for reactions of a *m*-xylyl diether tethered diporphyrin complex of rhodium(II) (·Rh(*m*-xylyl)Rh·) with H_2 and a series of methyl substrates CH_3R (R = H, CH_3, OH, C_6H_5). The initial substrate reactions occur exclusively through the intramolecular use of two rhodium(II) metalloradical centers followed by hydrogen atom transfer between Rh−H and Rh^{II}· sites. Preorganization of the four-centered transition state (M•···H···CH_3···•M) by ·Rh(*m*-xylyl)Rh· contributes to large rate enhancements for all of the substrate reactions relative to monometalloradical reactions[2] and improved kinetics as compared to a previously studied linear six-carbon diether tethered diporphyrin system.[3]

Results and Discussion

Hydrido, Alkyl, Benzyl, Hydroxyalkyl, and Rhodium(II) Derivatives of a *m*-Xylyl Tethered Dirhodium Diporphyrin.

Scheme 1

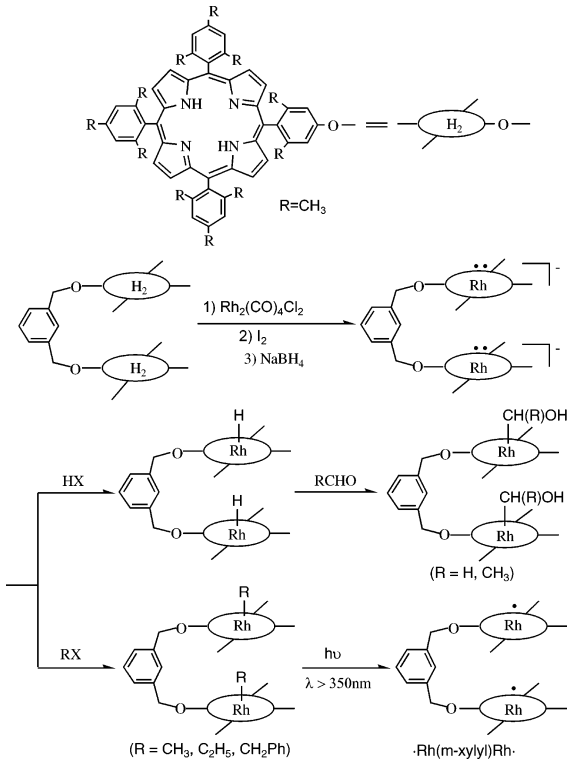

A series of hydride and organometallic derivatives of a *m*-xylyl diether tethered dirhodium diporphyrin that were generated by reported procedures[1−6,29,30] are outlined in Scheme 1.

The ^{1}H NMR shifts for the groups directly bonded to rhodium and the two CH_2 groups of the *m*-xylyl tether spacer group are summarized in Table 1 for a series of dirhodium diporphyrin derivatives. This set of ^{1}H NMR peaks permits identification of most dirhodium diporphyrin species in solution. The spacer CH_2 hydrogens are well separated from other ^{1}H NMR resonances and provide a particularly useful observable for kinetic and thermodynamic studies.

The dirhodium(II) derivative (·Rh(*m*-xylyl)Rh·) (**1**) is conveniently generated by photolysis of dialkyl dirhodium derivatives in benzene (Scheme 1). The porphyrin pyrrole hydrogens in **1** exhibit a downfield paramagnetic shift in the ^{1}H NMR spectrum that has an inverse temperature dependence characteristic of Curie paramagnetic behavior (Figure 1). Observation

(24) Fendrick, C. M.; Marks, T. J. *J. Am. Chem. Soc.* **1986**, *108*, 425.
(25) Walsh, P. J.; Hollander, F. J.; Bergman, R. G. *J. Am. Chem. Soc.* **1988**, *110*, 8729.
(26) Jones, W. D. *Acc. Chem. Res.* **2003**, *36*, 140.
(27) Churchill, D. G.; Janak, K. E.; Wittenberg, J. S.; Parkin, G. *J. Am. Chem. Soc.* **2003**, *125*, 1403.
(28) Periana, R. A.; Bergman, R. G. *J. Am. Chem. Soc.* **1986**, *108*, 7332.
(29) Zhang, X.-X.; Parks, G. F.; Wayland, B. B. *J. Am. Chem. Soc.* **1997**, *119*, 7938.
(30) Zhang, X.-X.; Wayland, B. B. *Inorg. Chem.* **2000**, *39*, 5318.

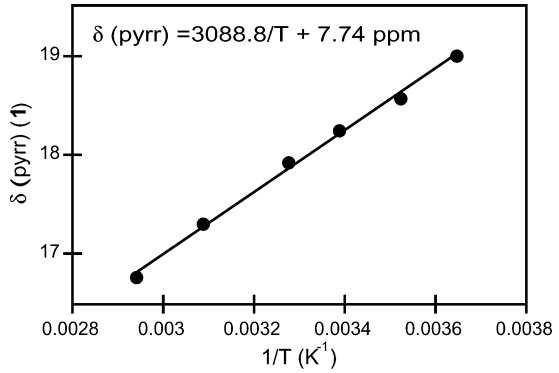

Figure 1. Temperature dependence for the pyrrole ^{1}H NMR paramagnetic shift of **1** in benzene-d_6.

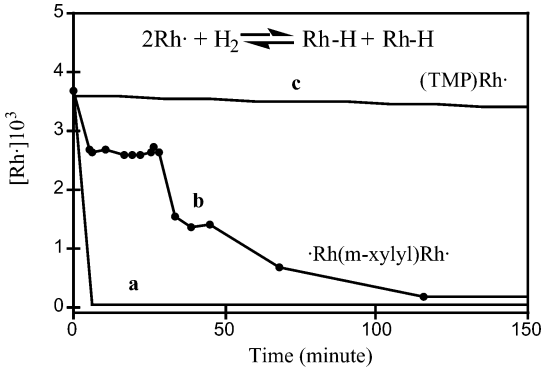

Figure 2. Change in the total molar concentration of rhodium(II) centers ([Rh·]) with time at 296 K for reaction with H_2: (a) $[\mathbf{1}]_i = 1.8 \times 10^{-3}$ M, $P_{H_2} = 250$ Torr; (b) $[\mathbf{1}]_i = 1.8 \times 10^{-3}$ M, $P_{H_2} = 30$ Torr; (c) $[(TMP)Rh\cdot]_i = 3.6 \times 10^{-3}$ M, $P_{H_2} = 250$ Torr.

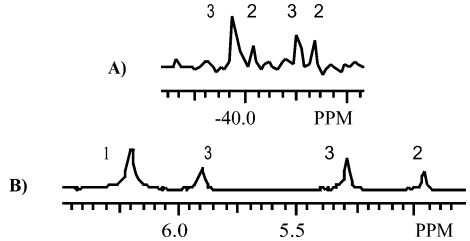

Figure 3. ^{1}H NMR spectra of the products for reaction of **1** with H_2 in C_6D_6 ($P_{H_2} = 30$ Torr) ($t = 5$ min) (**1** = ·Rh(*m*-xylyl)Rh·, **2** = H−Rh(*m*-xylyl)Rh−H, **3** = ·Rh(*m*-xylyl)Rh−H): (A) Rh−H region; (B) spacer $-CH_2-$ region.

of Curie paramagnetism demonstrates that **1** is a stable persistent bimetalloradical that does not dimerize even at low temperatures. The mesityl groups on the porphyrin unit prohibit the rhodium(II) sites from both intramolecular and intermolecular $Rh^{II}-Rh^{II}$ bonding, which is an important design feature of the porphyrin ligand. The spacer CH_2 groups in the paramagnetic dirhodium(II) complex (**1**) appear as a singlet that is shifted downfield by ~1.2 ppm (296 K) as compared to diamagnetic derivatives and provide a convenient means for identification and quantitative studies of the bimetalloradical (**1**) in solution (Table 1).

The dihydride derivative (H−Rh(*m*-xylyl)Rh−H) (**2**) in C_6D_6 has a characteristic Rh−*H* resonance ($\delta_{Rh-H} = -40.06$ ppm, $^1J_{103_{Rh-H}} = 42.5$ Hz) and a singlet spacer CH_2 resonance (δ_{CH_2}(**2**) = 4.99 ppm) (Table 1). The dihydride (**2**) in C_6D_6 evolves H_2 with formation of ·Rh(*m*-xylyl)Rh· (**1**) and the appearance of a second hydride derivative ·Rh(*m*-xylyl)Rh−H (**3**). Compound **3** (·Rh(*m*-xylyl)Rh−H) has a Rh−*H* resonance at −40.03 ppm ($^1J_{103_{Rh-H}} = 42.5$ Hz) and two spacer CH_2 peaks (δ_{CH_2}(**3**) = 5.90, 5.31 ppm) corresponding to the inequivalent sides of the tether. The tether CH_2 groups in **3** experience downfield paramagnetic shifts from the rhodium(II) site ($s = {}^1/_2$) relative to the diamagnetic dihydride (δ_{CH_2}(**2**) = 4.99 ppm). The sum of the paramagnetic shifts for the CH_2 groups in **3** relative to the diamagnetic dihydride (**2**) for the group proximal to rhodium(II) (0.91 ppm) and distal (0.32 ppm) is very close to the composite paramagnetic shift observed for the spacer in the bimetalloradical **1** (1.22 ppm) (Table 1), which provides a ^{1}H NMR criterion for species that contain one diamagnetic (Rh−X) and one paramagnetic (Rh^{II}·) site (·Rh(*m*-xylyl)Rh−X).

The dimethyl derivative (H_3C-Rh(*m*-xylyl)$Rh-CH_3$) (**4**) has a characteristic high field methyl resonance ($\delta_{Rh-CH_3} = -5.29$ ppm, $^2J_{103_{Rh-H}} = 2.9$ Hz) and a singlet spacer CH_2 peak (δ_{CH_2}(**4**) = 5.00 ppm). Photolysis of **4** ultimately results in the exclusive formation of the dirhodium(II) bimetalloradical complex (**1**), but early in the process a second methyl derivative assigned as ·Rh(*m*-xylyl)Rh−CH_3 (**5**) is observed by ^{1}H NMR spectroscopy (Table 1). Compound **5** has a characteristic high field resonance ($\delta_{Rh-CH_3} = -5.27$ ppm) and a set of proximal and distal spacer CH_2 resonances (δ_{CH_2}(**5**) = 5.90, 5.31 ppm) which are virtually indistinguishable from those in ·Rh(*m*-xylyl)Rh−H (**3**) (Table 1).

Reaction of ·Rh(*m*-xylyl)Rh· with Dihydrogen. Solutions of the ·Rh(*m*-xylyl)Rh· (**1**) in benzene when exposed to H_2 at 250 Torr or higher pressures react to form the diamagnetic dihydride complex H−Rh(*m*-xylyl)Rh−H (**2**) as the exclusive product during the time required to record the ^{1}H NMR spectrum (Figure 2a). The dihydride **2** is identified by ^{1}H NMR spectroscopy in solution through the Rh−*H* peak (−40.06 ppm, $^1J_{103_{Rh-H}} = 42.5$ Hz) and a single tether methylene ($-OCH_2-$) peak (4.99 ppm) (Table 1).

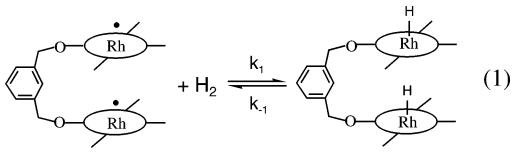

(1)

At 30 Torr of H_2 gas, the concentration of H_2 in benzene solution is less than the concentration of ·Rh(*m*-xylyl)Rh·. Because the reaction of **1** with H_2 is faster than the dissolution of H_2 from the gas, effectively all of the H_2 that is dissolved reacts away and the subsequent reaction becomes slow and dependent on the rate of dissolution of H_2 (Figure 2b). The two sharp decreases in the concentration of ·Rh(*m*-xylyl)Rh· shown in Figure 2b correspond to removing the sample from the NMR and shaking the tube to dissolve more H_2 and recording the ^{1}H NMR spectrum again. Solutions of **1** that have insufficient H_2 for the complete formation of **2** show the presence of a second hydride species **3** (·Rh(*m*-xylyl)Rh−H) (Figure 3).

The monohydride **3** is found to occur in equilibrium with the bimetalloradical **1** and dihydride **2** (eq 2) with an equilibrium constant close to 4 (K_2(296 K) = 4.1 ± 0.3). Idealized degenerate ($\Delta H_2^\circ = 0$) hydrogen atom transfer would give an equilibrium constant of 4 for reaction 2, and the observed K_2

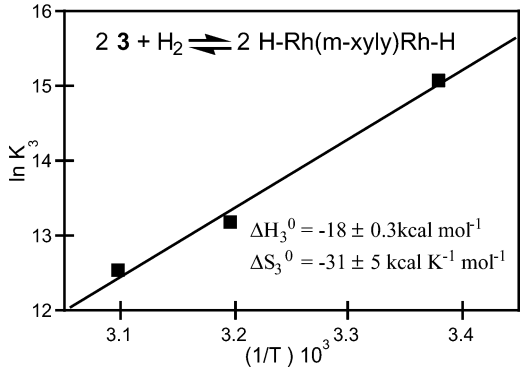

Figure 4. Van't Hoff plot for the reaction of **3** with H_2 to form H−Rh-(*m*-xylyl)Rh−H in C_6D_6 solution.

demonstrates that the Rh−H bond energies in H−Rh(*m*-xylyl)-Rh−H and ·Rh(*m*-xylyl)Rh−H must be the same.

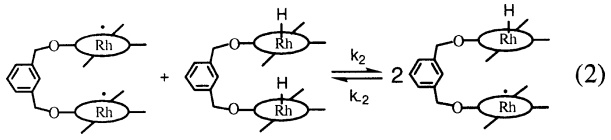

(2)

Reaction of **1** with H_2 at 20−30 Torr produces ^{1}H NMR observable equilibrium concentrations of **2** and **3**, which were used in conjunction with the molar concentration of H_2 in benzene to evaluate equilibrium constants for reaction 3. The temperature dependence of the equilibrium constants (K_3(323 K) = (2.8 ± 0.3) × 10^5; K_3(313 K) = (5.2 ± 0.5) × 10^5; K_3(296 K) = (3.5 ± 0.5) × 10^6) provides thermodynamic values for reaction 3 ($\Delta G_3°$(296 K) = −8.9 ± 0.5 kcal mol^{-1}; $\Delta H_3°$ = −18.0 ± 0.3 kcal mol^{-1}; $\Delta S_3°$ = −31 ± 5 cal K^{-1} mol^{-1}) (Figure 4).

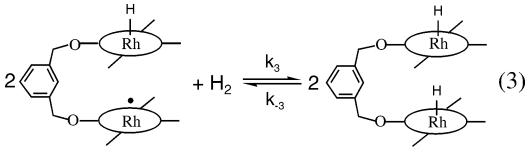

(3)

The forward rate constant (k_1(296 K)) for reaction 1 was evaluated at 90 Torr of H_2, where the excess H_2 in solution is directly observed by ^{1}H NMR spectroscopy. When benzene solutions of **1** are put in contact with 90 Torr of H_2, most of the reaction is over before the ^{1}H NMR spectrum can be recorded, but the final stage of the conversion of **1** to an equilibrium distribution of **2** and **3** with H_2 is observed. The reaction is too fast to obtain useful concentration versus time profiles, but the rate constant can be derived from the kinetic observations near the end of the process by assuming a mechanism involving reactions 1, 2, and 3. The forward rate constant for reaction 1 (k_1(296 K) = 40 ± 6 M^{-1} s^{-1}) was deduced by kinetic simulations aided by equilibrium constants determined for reactions 2 and 3 (K_2(296 K) = 4; K_3(296 K) = 3.5 × 10^6).

Reactions of ·Rh(*m*-xylyl)Rh· with CH_3−R (R = H, CH_3, OH, C_6H_5). Benzene solutions of ·Rh(*m*-xylyl)Rh· (**1**) react with the methyl C−H group of CH_3−R (R = H, CH_3, OH, C_6H_5) to produce H−Rh(*m*-xylyl)Rh−CH_2R as the initial product (eqs 4−7). Each of the initial C−H bond reactions is followed by a relatively fast near degenerate H atom transfer to **1** to form

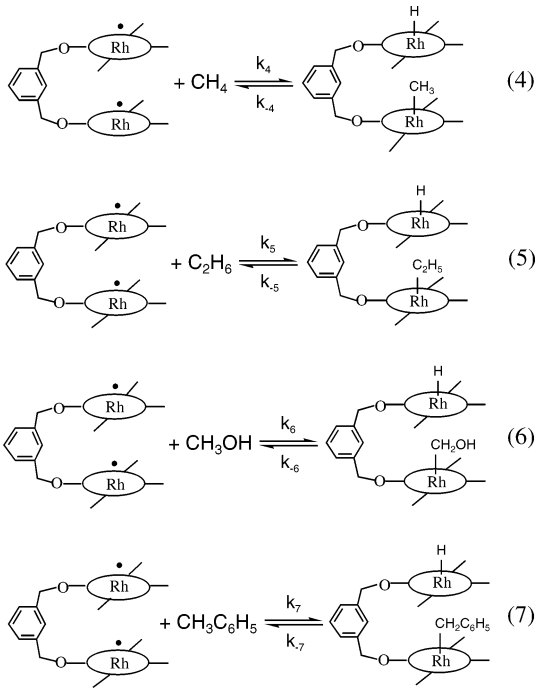

·Rh(*m*-xylyl)Rh−CH_2R and ·Rh(*m*-xylyl)Rh−H (eq 8). Subsequent very slow reactions carry the C−H bond reactions of **1** toward the ultimate formation of diorgano compounds (RCH_2−Rh(*m*-xyly)Rh−CH_2R) (eq 9) in a period of weeks to months.

·Rh(*m*-xylyl)Rh· + H−Rh(*m*-xylyl)Rh−CH_2R ⇌
·Rh(*m*-xylyl)Rh−H + ·Rh(*m*-xylyl)Rh−CH_2R (8)

·Rh(*m*-xylyl)Rh· + 2CH_3R →
RCH_2−Rh(*m*-xylyl)Rh−CH_2R + H_2 (9)

Kinetic studies for substrate reactions utilized the disappearance of the bimetalloradical **1** (·Rh(*m*-xylyl)Rh·) with time as the primary observable. The rate of disappearance of ·Rh(*m*-xylyl)Rh· depends on both the initial intramolecular substrate oxidative addition step and the subsequent hydrogen atom transfer (eqs 2, 8). Kinetic simulations including both the oxidative addition and the hydrogen transfer as reversible steps result in the rate constants for the fundamental forward oxidative addition step (k_{OA}) that are listed in Table 2. Rate constants for reactions of **1** with the deuterated substrates (CD_4, CD_3OD, $CD_3C_6D_5$) are also given in Table 2. The temperature dependence for the second-order rate constants derived for the initial substrate reaction step (rate = k_{OA}[·Rh(*m*-xylyl)Rh·][CH_3R]) yields activation parameters for the primary cleavage reaction (Table 2). Representative Eyring plots are shown in Figure 5 for the determination of the activation parameters for reactions of ·Rh(*m*-xylyl)Rh· with $CH_3C_6H_5$ and $CD_3C_6D_6$. Activation enthalpies for oxidative addition of H−CH_2R with two metal centers are relatively small ($\Delta H^‡ \approx$ 5−15 kcal mol^{-1}) and comparable to those for oxidative addition to single metal centers.[8,17b,31] The associative nature of the C−H bond reactions results in negative activation entropies (Table 2).

Each of the substrate C−H bond reactions with ·Rh(*m*-xylyl)-Rh·(**1**) (eqs 4−7) achieves a ^{1}H NMR observable equilibrium.

(31) Selmeczy, A. D.; Jones, W. D.; Osman, R.; Perutz, R. N. *Organometallics* **1995**, *14*, 5677.

Table 2. Rate Constants and Activation Parameters for the Oxidative Addition Step in the Substrate Reaction with ·Rh(*m*-xylyl)Rh· in C_6D_6 (296 K)

substrate	H_2	CH_4	CD_4	CH_3OH	CD_3OH	CH_3CH_3	$CH_3C_6H_5$	$CD_3C_6D_6$
k_{OA} (M^{-1} s^{-1})	40	8.3×10^{-2}	7.7×10^{-3}	1.03×10^{-2}	1.1×10^{-3}	3.3×10^{-4}	2.0×10^{-4}	4.0×10^{-5}
$\Delta G_{OA}^{\ddagger}$ (kcal mol^{-1})	15.2	18.8	20.2	20.0	21.3	22.0	22.3	23.3
$\Delta H_{OA}^{\ddagger}$ (kcal mol^{-1})		9.8 ± 0.5		15.6 ± 1.0			5.6 ± 0.5	7.6 ± 1.2
$\Delta S_{OA}^{\ddagger}$ (cal K^{-1} mol^{-1})		-31 ± 3		-15 ± 5			-56 ± 5	-53 ± 8

Table 3. Thermodynamic Values for Substrate Reactions of ·Rh(*m*-xylyl)Rh· and Derived Rh−H and Rh−CH_2R Bond Dissociation Enthalpies

substrate	H_2	CH_4	CH_3OH	CH_3CH_3	$CH_3C_6H_5$
H−X (kcal mol^{-1})	104.2	105.0	96.1	101.1	89.8
K (296 K)	$(3.5 \pm 0.5) \times 10^6$	$(8.0 \pm 0.2) \times 10^3$	$(1.5 \pm 0.5) \times 10^3$	80 ± 30	5.0 ± 0.5
$\Delta G°$ (kcal mol^{-1})	-8.9 ± 0.5	-5.4 ± 0.1	-4.3 ± 0.2	-2.6 ± 0.3	-1.0 ± 0.1
$\Delta H°$ (kcal mol^{-1})	-18.0 ± 0.3	-12.8 ± 1.5	-11.7 ± 1.5	-10.0 ± 1.5	-8.4 ± 1.5
Rh−X (kcal mol^{-1})	61.1 ± 0.4	56.7 ± 1.8	46.7 ± 1.8	50.0 ± 1.8	37.1 ± 1.8

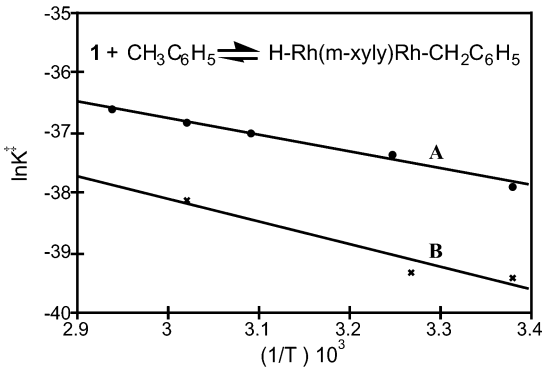

Figure 5. Determination of the activation parameters for reactions of toluene with ·Rh(*m*-xylyl)Rh· in C_6D_6: (A) $C_6H_5CH_3$: $\Delta H^{\ddagger} = 5.6 \pm 0.5$ kcal mol^{-1}; $\Delta S^{\ddagger} = -56 \pm 5$ cal K^{-1} mol^{-1}; (B) $C_6D_5CD_3$: $\Delta H^{\ddagger} = 7.6 \pm 1.2$ kcal mol^{-1}; $\Delta S^{\ddagger} = -53 \pm 8$ cal K^{-1} mol^{-1}.

Scheme 2

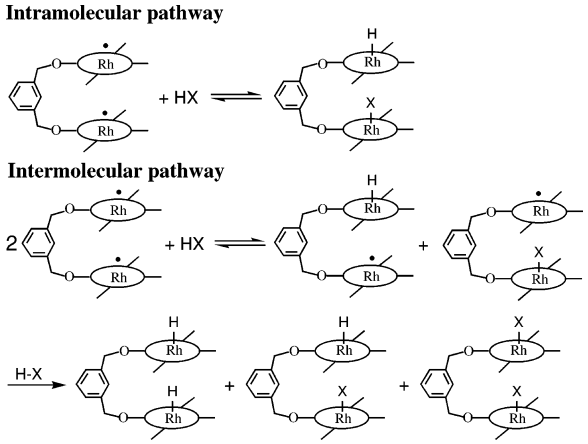

The substrate reactions are relatively fast and quickly achieve equilibrium that is maintained as the much slower subsequent reactions occur. Equilibrium constants at 296 K for reactions 4−7 were evaluated by integration of the ^1H NMR spectrum and are given in Table 3.

Bimetalloradical-Substrate Reaction Pathway from Product Studies. The most important mechanistic issue in the substrate reaction of the bimetalloradical complex (**1**) is whether the two metalloradical sites in the molecular unit are used in an intramolecular fashion in the fundamental substrate reaction step. The most direct way to address this mechanistic issue is by examination of the product(s) formed at each stage of the substrate reactions. When the two rhodium(II) centers in a bimetalloradical complex (**1**) react with a substrate H−X, the exclusive diamagnetic product is H−Rh(*m*-xylyl)Rh−X, but if rhodium(II) centers in different complexes react with H−X, then a 1:2:1 mixture of H−Rh(*m*-xylyl)Rh−H, H−Rh(*m*-xylyl)Rh−X, and X−Rh(*m*-xylyl)Rh−X will occur (Scheme 2). Observation of H−Rh(*m*-xylyl)Rh−X (X = CH_3, CH_2OH, CH_2CH_3, $CH_2C_6H_5$) as the exclusive diamagnetic product formed during the early stage for each substrate reaction clearly shows that the initial substrate H−X bond cleavage reactions involve two rhodium(II) centers from a single molecular unit (see Supporting Information).

The reaction pathway derived from observing the evolution of species in substrate C−H bond reactions of the bimetalloradical (**1**) (·Rh(*m*-xylyl)Rh·) is given in Scheme 3. Each of the methyl substrates (CH_3−R, R = H, CH_3, OH, and C_6H_5) reacts with ·Rh(*m*-xylyl)Rh· by a parallel series of events. The first step is a relatively fast substrate C−H bond cleavage reaction by the intramolecular use of two Rh^{II}· sites in ·Rh(*m*-xylyl)Rh· that forms H−Rh(*m*-xylyl)Rh−CH_2R as the exclusive product (Stage I, eq 1, Scheme 3). Subsequent fast degenerate hydrogen atom transfer reactions occur beginning with H· transfer from H−Rh(*m*-xylyl)Rh−CH_2R to ·Rh(*m*-xylyl)Rh· (Stage II, eq 2). The reactions in Stages I and II are relatively fast, and the species present achieve an equilibrium distribution, which is maintained as much slower intermolecular substrate reactions carry the reaction toward completion. Reductive elimination of H_2 (Stage III, eqs 5,6) opens a site for slow intermolecular substrate reactions to move the system toward the ultimate diamagnetic diorgano products (RCH_2−Rh(*m*-xylyl)Rh−CH_2R) and H_2 (Stage IV, eqs 9,10).

Activation Parameters. One of the primary initial motivations for constructing bimetalloradical reagents was to attempt to convert the termolecular processes observed for (TMP)Rh^{II}· (rate = k[(TMP)Rh^{II}·]^2[S]) into bimolecular pathways through the intramolecular use of two Rh^{II}· centers (rate = k[·Rh(*m*-xylyl)Rh·][S] and also reduce the activation entropy associated with three molecules in the transition state.[3,4] Kinetic studies and product analysis demonstrate that bimolecular substrate reactions with large rate enhancements are obtained, but the observed activation entropies are more complicated. Termolecular reactions of (TMP)Rh^{II}· with CH_4 and H_2 have activation entropies of about −40 cal K^{-1} mol^{-1},[2,21] and the observation of a smaller $\Delta S^{\ddagger}$ value for reactions of ·Rh(*m*-xylyl)Rh· with

Scheme 3. Substrate C−H Bond Reaction Pathway

I. Intramolecular Substrate Activation (reversible Oxidative Addition/Reductive Elimination)

1) ·Rh(m-xylyl)Rh· + H-CH_2R $\underset{k_{RE}}{\overset{k_{OA}}{\rightleftharpoons}}$ H-Rh(m-xylyl)Rh-CH_2R

II. Hydrogen Atom Transfer between Rh Centers

2) ·Rh(m-xylyl)Rh· + H-Rh(m-xylyl)Rh-CH_2R $\overset{k_{HT}}{\rightleftharpoons}$ H-Rh(m-xylyl)Rh· + ·Rh(m-xylyl)Rh-CH_2R

3) 2 H-Rh(m-xylyl)Rh· $\rightleftharpoons$ ·Rh(m-xylyl)Rh· + H-Rh(m-xylyl)Rh-H

4) H-Rh(m-xylyl)Rh· + H-Rh(m-xylyl)Rh-CH_2R $\rightleftharpoons$ H-Rh(m-xylyl)Rh-H + ·Rh(m-xylyl)Rh-CH_2R

III. Reductive Elimination of H_2

5) H-Rh(m-xylyl)Rh-H $\rightleftharpoons$ ·Rh(m-xylyl)Rh· + H_2

6) 2 H-Rh(m-xylyl)Rh-CH_2R $\rightleftharpoons$ 2 ·Rh(m-xylyl)Rh-CH_2R + H_2

IV. Intermolecular Substrate Activation (reversible Oxidative Addition/Reductive Elimination)

7) 2 ·Rh(m-xylyl)Rh· + H-CH_2R $\rightleftharpoons$ H-Rh(m-xylyl)Rh· + ·Rh(m-xylyl)Rh-CH_2R

8) 2 H-Rh(m-xylyl)Rh· + H-CH_2R $\rightleftharpoons$ H-Rh(m-xylyl)Rh-H + H-Rh(m-xylyl)Rh-CH_2R

9) 2 ·Rh(m-xylyl)Rh-CH_2R + H-CH_2R $\rightleftharpoons$ H-Rh(m-xylyl)Rh-CH_2R + RCH_2-Rh(m-xylyl)Rh-CH_2R

10) H-Rh(m-xylyl)Rh· + ·Rh(m-xylyl)Rh-CH_2R + H-CH_2R $\rightleftharpoons$ H-Rh(m-xylyl)Rh-H + RCH_2-Rh(m-xylyl)Rh-CH_2R

11) H-Rh(m-xylyl)Rh· + ·Rh(m-xylyl)Rh-CH_2R + H-CH_2R $\rightleftharpoons$ 2 H-Rh(m-xylyl)Rh-CH_2R

CH_4 ($\Delta S^{\ddagger} = -31$ cal K^{-1} mol^{-1}) and CH_3OH ($\Delta S^{\ddagger} = -15$ cal K^{-1} mol^{-1}) fulfilled the expected change in $\Delta S^{\ddagger}$ for a bimolecular reaction. However, the toluene reaction with **1** has an unusually small activation enthalpy and an exceptionally large negative activation entropy ($\Delta H^{\ddagger} = 5.6 \pm 0.5$ kcal mol^{-1}; $\Delta S^{\ddagger} = -56 \pm 5$ cal K^{-1} mol^{-1}). The activation entropy is in the range expected for termolecular processes, but both product analysis and kinetic studies indicate that the toluene reaction is bimolecular with a rate that is first order in both ·Rh(*m*-xylyl)-Rh· and toluene. The origin of the large $\Delta S^{\ddagger}$ ($\Delta S^{\ddagger} = -56 \pm 5$ cal K^{-1} mol^{-1}) is tentatively associated with inhibition of internal modes of motion in the transition state. A plot of $\Delta H^{\ddagger}$ versus $-T\Delta S^{\ddagger}$ indicates that the activation entropy and activation enthalpy are correlated and substantially compensating (Figure 6). The toluene reaction apparently achieves a minimum $\Delta G^{\ddagger}$ and thus a maximum rate through a transition state structure that gives a low activation enthalpy along with large compensating entropy losses. A structure that has constrained internal motions but achieves a minimum $\Delta G^{\ddagger}$ by favorable electronic activation could account for the observation.

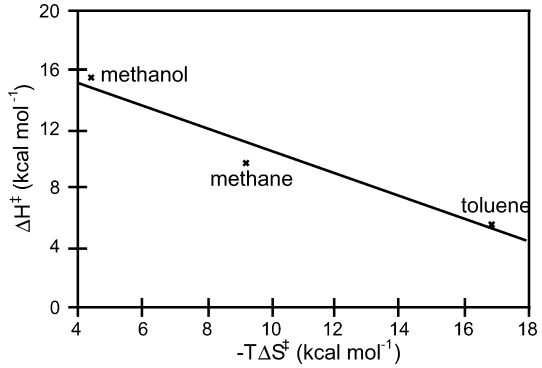

Figure 6. Plot of $\Delta H^{\ddagger}$ versus $-T\Delta S^{\ddagger}$ for the substrate C−H activation by ·Rh(*m*-xylyl)Rh· in C_6D_6.

Kinetic Isotopic Effects on Rhodium(II) Porphyrin Metalloradical Reactions of Hydrocarbons. Kinetic and equilibrium deuterium isotope effects (k_H/k_D; K_H/K_D) for reactions of hydrocarbons with metal centers and M=X units are complicated by a series of contributions that arise from factors such as intermediate metal−hydrocarbon complexes,[26−28,32] a multiplicity of isotope sensitive vibrations[32] and tunneling, in addition to the conventional dominant contribution from the zero point energy changes associated with conversion of one vibration into the reaction coordinate.[33] The overall isotope effect for an oxidative addition to a metal or reductive elimination from a metal complex is usually small[8c,10b,34,35] or inverse[28,36−40] and is often a composite isotope effect that results from a series of fundamental events involving intermediate hydrocarbon complexes.[26,27] Addition of a hydrocarbon C−H bond across a

(32) Slaughter, L. M.; Wolczanski, P. T.; Klinckman, T. R.; Cundari, T. R. *J. Am. Chem. Soc.* **2000**, *122*, 7953.
(33) (a) Melander, L.; Saunders, W. H., Jr. *Reaction Rates of Isotopic Molecules*; Wiley-Interscience: New York, 1980. (b) Lowry, T. H.; Richardson, K. S. *Mechanism and Theory in Organic Chemistry*, 3rd ed.; Harper & Row: New York, 1987. (c) Carpenter, B. K. *Determination of Reaction Mechanisms*; Wiley-Interscience: New York, 1984. (d) *Isotope Effects in Chemical Reactions*; Collins, C. J., Bowman, N. S., Eds.; ACS Monograph No. 167; Van Nostrand Reinhold Co.: New York, 1970.
(34) Harper, T. G. P.; Shinomoto, R. S.; Deming, M. A.; Flood, T. C. *J. Am. Chem. Soc.* **1988**, *110*, 7915.
(35) (a) Bengali, A. A.; Schultz, R. H.; Moore, C. B.; Bergman, R. G. *J. Am. Chem. Soc.* **1994**, *116*, 9585. (b) Schultz, R. H.; Bengali, A. A.; Tauber, M. J.; Weiller, B. H.; Wasserman, E. P.; Kyle, K. R.; Moore, C. B.; Bergman, R. G. *J. Am. Chem. Soc.* **1994**, *116*, 7369.
(36) Buchanan, J. M.; Stryker, J. M.; Bergman, R. G. *J. Am. Chem. Soc.* **1986**, *108*, 1537.
(37) Bullock, R. M.; Headford, C. E. L.; Hennessy, K. M.; Kegley, S. E.; Norton, J. R. *J. Am. Chem. Soc.* **1989**, *111*, 3897.
(38) (a) Parkin, G.; Bercaw, J. E. *Organometallics* **1989**, *8*, 1172. (b) Stahl, S. S.; Labinger, J. A.; Bercaw, J. E. *J. Am. Chem. Soc.* **1996**, *118*, 5961.
(39) Gould, G. L.; Heinekey, D. M. *J. Am. Chem. Soc.* **1989**, *111*, 5502.
(40) Wang, C.; Ziller, J. W.; Flood, T. C. *J. Am. Chem. Soc.* **1995**, *117*, 1647.

M=X[17b,32] unit can produce a wide range of isotope effects and is capable of giving exceptionally large kinetic isotope effects that arise from many isotope-sensitive vibrations[17b,32] and possible contributions from tunneling.

Deuterium kinetic isotope effects for the reaction of (TMP)Rh^{II}· with methane are large, but they occur in the normal range and the temperature dependence is consistent with the value expected for conversion of a C−H stretching mode in the transition state (k_H/k_D(296 K) = 8.2; k_H/k_D(353 K) = 5.1; $\Delta H^{\ddagger}_{(D)} - \Delta H^{\ddagger}_{(H)} \approx 1.2$ kcal mol^{-1}).[33] These results suggested that the kinetic isotope effects for the reaction of (TMP)Rh^{II}· with CH_4/CD_4 may be interpretable in terms of the conventional zero point energy arguments.[33] The values of k_H/k_D for methane with (TMP)Rh^{II}· are comparable to those observed for hydrogen atom abstractions by radicals (X·) from methane (k_H/k_D(296 K) ≈ 9),[41,42] which proceed through a linear three-centered transition state (X•···H···CH_3). Similarity in the observed kinetic isotope effects contributed to the proposal of a near linear symmetrical four-centered transition state (Rh•···H···CH_3···•Rh) for the reaction of methane with (TMP)Rh^{II}· in analogy with the linear three-centered transition state for atom abstractions (X•···H···CH_3). Both of these transition states have a related linear X•···H···C unit that would produce comparable isotope effects if loss of a C−H stretching vibration were the dominant contribution.

Relatively large kinetic isotope effects are observed for each of the substrate reactions of ·Rh(*m*-xylyl)Rh· that were studied (296 K) ($k_H/k_D(CH_4)$ = 10.8 ± 1.0; $k_H/k_D(CH_3OH)$ = 9.7 ± 0.8; $k_H/k_D(CH_3C_6H_5)$ = 5.0 ± 0.7). Temperature dependence of k_H/k_D for the toluene reaction with **1** gives a change in activation enthalpy ($\Delta H_{(D)}{}^{\ddagger} - \Delta H_{(H)}{}^{\ddagger} \approx 2$ kcal mol^{-1}) (Figure 5) that is consistent with the dominance of the zero point energy terms.[33] The range of k_H/k_D values and the temperature dependence of the isotope effects for the bimetalloradical reactions are comparable to those previously observed for the (TMP)Rh^{II}· system,[2] which is consistent with the mono- and bimetalloradical substrate reactions utilizing closely related transition states. The electronic properties of square-planar rhodium(II) and the rigid sterically demanding porphyrin ligand combine to restrict the accessible reaction pathways and guide the concerted metalloradical C−H bond reactions through a near linear symmetrical four-centered transition state.

Equilibrium Thermodynamics for Substrate Reactions of ·Rh(*m*-xylyl)Rh·. Equilibrium constants and standard free energy changes for the reactions of H_2 and CH_3R with ·Rh(*m*-xylyl)Rh· are given in Table 3. The temperature dependence of the equilibrium constants for the H_2 reaction (eq 3) gives the enthalpy and entropy changes for reaction 3 ($\Delta H_3° = -18.0 \pm 0.3$ kcal mol^{-1}; $\Delta S_3° = -31 \pm 5$ cal K^{-1} mol^{-1}). Enthalpy changes ($\Delta H°$) for reactions of **1** with CH_4, CH_3CH_3, CH_3OH, and $CH_3C_6H_5$ were estimated from the measured free energy changes ($\Delta G°$ (296 K)) and assuming that the entropy change ($\Delta S°$) for this type of process in benzene is in the range of −25 ± 5 cal K^{-1} mol^{-1} [1,23b,43] ($T\Delta S° = 7.4 \pm 1.5$ kcal mol^{-1}, T = 296 K) (Table 3).

The enthalpy change in the H_2 reaction with **1** can be expressed in terms of bond dissociation enthalpies (BDE) ($\Delta H_3°$ = (H−H) − 2 (Rh−H) = −18.0 kcal mol^{-1}). Evaluating this expression using 104.2 kcal mol^{-1} for the H−H BDE[44] gives a Rh−H BDE of 61.1 ± 0.4 kcal mol^{-1} (Table 3). The Rh−H BDE value of 61.1 ± 0.4 kcal mol^{-1} determined from this equilibrium measurement is highly reliable because it depends only on the H−H BDE that is accurately known. This is an important (por)Rh−H BDE determination because it is more direct than prior measurements that were dependent both on the Rh−Rh BDE values estimated from kinetic measurements[45] and on the H−H BDE. The accurate measurement of a Rh−H BDE of 61.1 ± 0.4 kcal mol^{-1} in H−Rh(*m*-xylyl)Rh−H provides confidence that prior estimates of Rh−H BDE values for (OEP)Rh−H (62 kcal mol^{-1}),[45] (TMP)Rh−H (60 kcal mol^{-1}),[2] and (F_{28}TPP)Rh−H (58 kcal mol^{-1})[5] are reliable and thus validates many additional (por)Rh−X[1,45,46] bond dissociation enthalpies that were evaluated relative to the BDE for the (por)Rh−H species.

The $\Delta H°$ values for the C−H bond reactions (·Rh(*m*-xylyl)Rh· + H−CH_2R ⇌ H−Rh(*m*-xylyl)Rh−CH_2R) also can be expressed in terms of bond energies ($\Delta H°$ = (H−CH_2R) − (Rh−H) − (Rh−CH_2R)). Using recently tabulated substrate C−H bond dissociation enthalpies (kcal mol^{-1})[44] (H−CH_3 (105.0); H−CH_2CH_3 (101.1); H−CH_2OH (96.1); H−$CH_2C_6H_5$ (89.8)) and 61.1 ± 0.4 kcal mol^{-1} for the Rh−H BDE yields the set of derived Rh−organo BDE values given in Table 3 (Rh−CH_3 (56.7 ± 1.8 kcal mol^{-1}); Rh−CH_2CH_3 (50.0 ± 1.8 kcal mol^{-1}); Rh−CH_2OH (46.7 ± 1.8 kcal mol^{-1}); Rh−$CH_2C_6H_5$ (37.1 ± 1.8 kcal mol^{-1})).

The order of thermodynamic favorability for C−H bond reactions of CH_3R with ·Rh(*m*-xylyl)Rh· is $CH_4 > CH_3OH > CH_3CH_3 > CH_3C_6H_5$. Oxidative addition of CH_4 to **1** is most favorable ($\Delta G° = -5.4 \pm 0.1$ kcal mol^{-1}), but the total range of $\Delta G°$ for this set of substrate C−H bond reactions is only 4.4 kcal mol^{-1}. The large difference in substrate C−H bond dissociation enthalpies (CH_4 (105.0); $CH_3C_6H_5$ (89.8)) gives the impression that methane is much more difficult to activate than other alkanes. However, the difference in Rh−CH_2R bonds energies (Rh−CH_3 (56.7); Rh−$CH_2C_6H_5$ (37.1)) more than compensates for the difference in H−CH_2R values, resulting in a thermodynamic preference for methane activation. Thermodynamic preference for C−H bond reactions of methane as compared to other alkanes has been widely observed and should be a general result for oxidative addition of hydrocarbons to metal centers.[8a,9c,17,47] Jones has shown that alkane and aromatic hydrocarbons that have the largest C−H bond energies are the most easily activated for oxidative addition to metal complexes.[9c] This general result occurs because the order of increasing M−C bond dissociation energies is the same as the C−H bond energies, but the differences between the M−C bond energies are substantially larger than the differences between C−H bond energies.

The (por)Rh−CH_2R bond dissociation energies (BDE) derived for the series of complexes (R = H, CH_3, OH, C_6H_5) have a near linear variation with the H−CH_2R BDE (Figure 7). Differences in the H−CH_2R BDEs are dominated by the

(41) Johnston, H. S. *Gas-Phase Reaction Rate Theory*; The Ronald Press Co.: New York, 1966; p 239.
(42) Chiltz, G.; Eckling, R.; Goldfinger, P.; Huybrechts, G.; Johnston, H. S.; Meyers, L.; Verbeke, G. *J. Chem. Phys.* **1963**, *38*, 1053.
(43) Wayland, B. B.; Feng, Y.; Ba, S. *Organometallics* **1989**, *8*, 1438.
(44) Blanksby, S. J.; Ellison, G. B. *Acc. Chem. Res.* **2003**, *36*, 255.
(45) Wayland, B. B.; Coffin, V. L.; Farnos, M. D. *Inorg. Chem.* **1988**, *27*, 2745.
(46) Wayland, B. B. *Polyhedron* **1988**, *7*, 1545.
(47) Stoutland, P. O.; Bergman, R. G.; Nolan, S. P.; Hoff, C. D. *Polyhedron* **1988**, *7*, 1429.

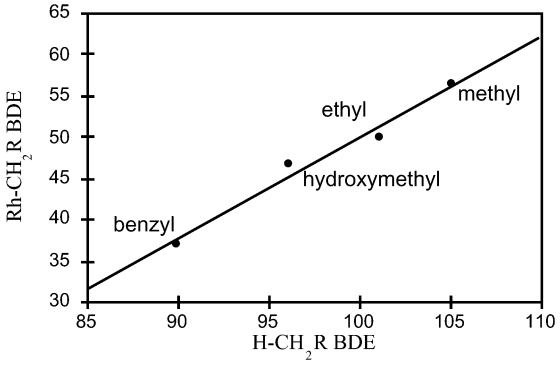

Figure 7. Plot of (por)Rh−CH_2R versus H−CH_2R bond dissociation enthalpies (kcal mol^{-1}).

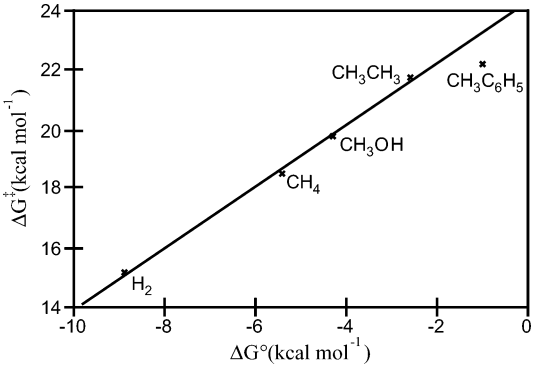

Figure 8. Plot of $\Delta G^{\ddagger}$ versus $\Delta G°$ for substrate reaction of ·Rh(*m*-xylyl)Rh· at 296 K.

differences in the radical stabilization energies, which make the same contribution to the Rh−CH_2R and H−CH_2R BDEs. The difference between the Rh−CH_3 and Rh−$CH_2C_6H_5$ BDEs of ∼20 kcal mol^{-1} is ∼5 kcal mol^{-1} larger than the difference between the H−CH_3 and H−$CH_2C_6H_5$ BDEs (∼15 kcal mol^{-1}), even though the absolute values of the Rh−CH_2R BDEs (37−57 kcal mol^{-1}) are much less than the H−CH_2R values (90−105 kcal mol^{-1}). The larger spread in Rh−CH_2R BDEs must result from an interaction that weakens the Rh−CH_2R bond but does not affect the H−CH_2R bond energy. The origin of this energy term is most probably a repulsion term between electrons of the (por)Rh unit and the CH_2R fragments which is synonymous with a steric effect. The order of decreasing $-\Delta G°$ and $-\Delta H°$ values for the CH_3R substrate reactions parallels the expected order of increasing steric effects (CH_4 < CH_3OH < CH_3CH_3 < $CH_3C_6H_5$). Differences in steric interactions probably dominate the relatively small differences in the substrate reaction thermodynamics, and the stabilization energy for ·CH_2R radicals dominates the difference in the Rh−CH_2R BDEs (Figure 7). The use of C−H BDEs to anticipate relative rates of C−H bond reactions also could be misleading because hydrogen atom abstractions are the only reactions where the C−H BDE values are directly related to the activation parameters.

Activation free energies ($\Delta G^{\ddagger}$) for the substrate reactions with ·Rh(*m*-xylyl)Rh· are found to decrease regularly as the thermodynamic free energy changes ($\Delta G°$) become more favorable (Figure 8; Tables 2,3). A plot of $\Delta G^{\ddagger}$ versus $\Delta G°$ for reactions of **1** with H_2, CH_4, C_2H_6, and CH_3OH indicates a near linear relationship with a slope close to unity ($\Delta(\Delta G^{\ddagger})/\Delta(\Delta G°)$ = 1.05), which establishes criteria for normal substrate behavior in this system (Figure 8). The toluene reaction with **1** has the least favorable $\Delta G°$ and the least favorable $\Delta G^{\ddagger}$, which fits into the general qualitative trend in $\Delta G^{\ddagger}$ versus $\Delta G°$. However, the toluene methyl C−H bond reaction deviates from the quantitative correlation of $\Delta G^{\ddagger}$ versus $\Delta G°$ toward lower $\Delta G^{\ddagger}$ by ∼1 kcal mol^{-1}, which suggests that toluene reacts somewhat faster than would be expected from comparison with the other substrates (Figure 8). Interaction of the phenyl π with a methyl carbon p orbital could provide electronic stabilization for the transition state that is largely compensated for by entropy changes from steric constraints of the phenyl group, but produces a modest net rate enhancement for the toluene reaction.

Summary and Conclusion

A tethered dirhodium(II) diporphyrin complex reacts as a bimetalloradical and gives large rate enhancements for H−H and H−CH_2R substrate reactions relative to monorhodium(II) metalloradicals. The bimetalloradical ·Rh(*m*-xylyl)Rh· reacts to form products that reflect total regioselectivity for alkyl C−H groups in preference to O−H and C−C bonds and with complete exclusion of aromatic C−H bond reactions. The products formed as the reactions proceed to equilibrium are uniquely consistent with the intramolecular use of two Rh^{II}· centers in the alkyl C−H bond reactions of methane, ethane, methanol, and toluene. The substrate alkyl group activation process occurs by relatively fast reaction of ·Rh(*m*-xylyl)Rh· with the substrate (CH_3R) to form H−Rh(*m*-xylyl)Rh−CH_2R followed by a moderately fast hydrogen atom transfer from a Rh−H center to ·Rh(*m*-xylyl)Rh· forming ·Rh(*m*-xylyl)Rh−H and ·Rh(*m*-xylyl)Rh−CH_2R. Reversible hydrogen atom transfer between Rh−H and Rh^{II}· centers establishes equilibria that ensure the presence of ·Rh(*m*-xylyl)Rh· for substrate reaction until effectively all of the Rh^{II}· sites have reacted away.

The second-order rate constants and the equilibrium constants (296 K) for the substrate reactions with ·Rh(*m*-xylyl)Rh· decrease in the order of H_2 > CH_4 > CH_3OH > CH_3CH_3 > $CH_3C_6H_5$. Equilibrium constant measurements give an absolute Rh−H bond dissociation enthalpy (BDE) of 61.1 ± 0.4 kcal mol^{-1} and estimates of BDE values for Rh−CH_2R units (R = H (56.7 ± 1.8 kcal mol^{-1}); CH_3 (50.0 ± 1.8 kcal mol^{-1}); OH (46.7 ± 1.8 kcal mol^{-1}); C_6H_5 (37.1 ± 1.8 kcal mol^{-1})). Differences in the Rh−CH_2R bond dissociation enthalpies correlate linearly with the C−H BDEs because both are dominated by differences in the ·CH_2R radical stability. The sequence of decreasing thermodynamically favorable $\Delta G°$ values for substrate reactions corresponds to the order of increasing steric requirements (H_2 < CH_4 < CH_3OH < CH_3CH_3 < $CH_3C_6H_5$). The activation free energy ($\Delta G^{\ddagger}$) decreases regularly as the $\Delta G°$ for the substrate reactions becomes more favorable.

Activation parameters and deuterium isotope effects are consistent with an approximately linear four-centered transition state that directs a low activation enthalpy pathway for substrate (H−X) bond cleavage. The linear four-centered transition state provides a metalloradical reaction pathway that is complementary to the three- and the four-centered cyclic transition states associated by C−H bond reaction with single metal centers and M=X units, respectively. Each of these reaction pathways provides a concerted low activation energy route for C−H bond cleavage, but the transition state structures and steric and

electronic properties of the metallo-species can produce different properties, such as kinetic isotope effects and substrate selectivities. Facile alkane hydrocarbon reactions with complete exclusion of aromatic C−H bond reactions are currently a unique selectivity feature of rhodium(II) porphyrins that results from the combined structural and electronic features of the substrate, metal complex, and transition state.

Experimental Section

General Methods. All manipulations were performed on a high-vacuum line equipped with a Welch Duo-Seal vacuum pump. ^{1}H NMR spectra were obtained on a Bruker AC-360 or Bruker interfaced to an Aspect 3000 computer or Bruker DMX-300 to a SGI computer controlled at ambient temperature. Variable-temperature ^{1}H NMR spectra were obtained on an IBM-Bruker spectrometer equipped with a Bruker VT-1000 or VT-2000 temperature controller. The probe was cooled with a FTS system refrigerator unit equipped with a temperature controller. All spectra were referenced using the residual solvent peak as an internal standard (benzene-d_6, $\delta = 7.155$ ppm; toluene-d_8, $\delta =$ 2.09 ppm). All temperatures for variable-temperature NMR spectroscopy were calibrated relative to the chemical shift differences in the ^{1}H NMR spectra of known standards ethylene glycol with a trace (0.03% v/v) of concentrated aqueous HCl acid for high temperature (295−415 K), and methanol with an added trace (0.03% v/v) of concentrated aqueous HCl acid for low temperature (265−313 K). The samples were protected from light prior to and during the experiments. Fast atom bombardment mass spectrometry (FAB-MS) analysis was carried out on a VG70SE double focus magnetic sector spectrometer operating at 7 kV. The sample was dissolved in benzene and then into nitrobenzyl alcohol matrix and then ionized by a 35 kV Cs ion beam.

Reagents. NMR solvents (C_6D_6 and C_7D_8) were purchased from Cambridge Isotope Lab, dried over 4 Å molecular sieves, and degassed by freeze−pump−thaw cycles to remove oxygen. Chloroform and 1,2-dichloroethane used in the synthetic procedures were purified by washing three times with water followed by chromatography on grade 1 alumina for the removal of ethanol and water.

Gases. The prepurified H_2 (99.99%) gas was purchased from Scott Specialty Gas., Inc. Research grade methane and ethane gases were commercially obtained from Matheson. CD_4 was purchased from MSD Isotopes and purified by vacuum transferring the contents of the bulb provided by MSD to a new bulb coated with a potassium film. The potassium film was created by gently heating small pieces of potassium metal in the bulb under vacuum.

Kinetic-Mechanistic and Thermodynamic Studies. Reactions of hydrocarbons and H_2 with ·Rh(*m*-xylyl)Rh· (**1**) were carried out in the controlled atmosphere valve NMR tubes. A stock solution of dimethyl dirhodium(III) diporphyrin complex **4** in benzene was prepared with known concentration. The initial concentration of **1** was determined by the aliquot of the stock solution taken for each sample. The sample solutions were frozen by dry ice/acetone before they were put into the magnet, and the time was recorded. A computer program was used to control the number of scans and the intervals between acquisitions in the ^{1}H NMR spectra. Each experiment was recorded synchronously in time and ^{1}H NMR spectra immediately after the solution was well mixed. Error in recording the time can be up to 30 s. The absolute concentration of the unreacted species **1** in the reacting system was determined by comparing the integrated intensity of the tether hydrogen resonance (−OCH_2− at 6.20 ppm) of **1** to the sum of all tether hydrogen resonances (from 6.20 to 4.99 ppm). The NMR samples for the kinetic studies at variable temperature were kept in the probe of the magnet for continuous observation until the dirhodium(II) species was no longer observed. Kinetics for each experiment were observed for at least 6 half-lives. Simulation of the concentration versus time profiles was obtained by use of the computer software KaleidaGraph and MacKinetics.[48]

Concentrations of Substrates in Benzene. The molar concentration of dihydrogen in benzene-d_6 as a function of temperature and the hydrogen pressure is given by the following expression: $[H_2] = [(2.3421 \times 10^{-3}) + (2.2592 \times 10^{-5})(T_2(°C))][T_2(K) \times P_1(Torr)/T_1(K)][1/760(Torr)]$, where T_1 and P_1 are the temperature and pressure at which the sample is prepared and T_2 is the temperature at which the experiment is performed.[49] For methane gas, the temperature and pressure dependence of the molar concentration are expressed as: $[CH_4]_{T,P} = [3.871 \times 10^{-2}\ \text{mol L}^{-1} - (5.143 \times 10^{-5})T_2](T_2/T_1)(P(atm))$, where P is the CH_4 pressure in atmospheres at temperature T_1 (296 K) and T_2 is the temperature at which the experiment is performed. Solubility data were taken from Evans and Battino,[50] and the temperature dependence of the density of benzene was from Brunel and VanBibber.[51] The solubility of CD_4 in benzene was assumed to be the same as that of CH_4. The pressure dependence (30−350 Torr) of the ethane concentration in C_6D_6 at room temperature ($T = 296$ K) was measured by the integration of the ethane peak (0.80 ppm) to that of the internal standard peak-methyl on hexamethylbenzene at 2.13 ppm with known concentration. The ethane concentration relationship is expressed as: $[C_2H_6]_P = (1.807 \times 10^{-4} \times P_{C_2H_6}(Torr))(mol/L)$.

The concentrations of the liquid substrates (methanol and toluene) were determined by weighing the sample before and after the substrate was vacuum-transferred. Pure toluene-d_8 that has a concentration of 9.41 M at 296 K was used both as solvent and as substrate for the activation studies.

Acknowledgment. This research was supported by the Department of Energy, Division of Chemical Sciences, Office of Science through grant DE-FG02-86ER-13615.

Supporting Information Available: Synthetic details, complete ^{1}H NMR data for compounds **1**−**15**, kinetic observations for reactions 4−7, and determination of activation parameters for reactions 4, 5, and 7. This material is available free of charge via the Internet at http://pubs.acs.org.

JA049291S

(48) MacKinetics, written by and obtained from Leipold, W. S., III; Weiher, J. F.; McKinney, R. J. E. I. Du pont de Nemours, Inc., 1992−1995.
(49) Farnos, M. D. Ph.D. Thesis, University of Pennsylvania, 1986.
(50) Evans, F. D.; Battino, R. *J. Chem. Thermodyn.* **1971**, *3*, 753.
(51) Brunel, R. F.; VanBibber, K. *Int. Crit. Tables* **1928**, *3*, 27.